

Pd^{II} and Pt^{II} Complexes with Amphiphilic Ligands: Formation of Micelles and [5]Rotaxanes with α -Cyclodextrin in Aqueous Solution

Toshiaki Taira, Yuji Suzaki, and Kohtaro Osakada*^[a]

Abstract: [3]Pseudorotaxanes [1(α -CD)₂][X] (X = Cl, NO₃), prepared from reaction of an *N*-alkylbipyridinium [4,4'-bpy-*N*-(CH₂)₁₀OC₆H₃-3,5-(OMe)₂][X] ([1][X]) and α -CD, react with M-(NO₃)₂(en) (M = Pd, Pt; en = 1,2-ethylenediamine) in a 2:1 molar ratio to afford [5]rotaxanes [M{(4,4'-bpy-*N*-(CH₂)₁₀OC₆H₃-3,5-(OMe)₂)(α -CD)₂}(en)][NO₃]₄ ([2(α -CD)₄][NO₃]₄, M = Pd; [3(α -CD)₄][NO₃]₄, M = Pt). A similar reaction of [1][Cl] with [M(NO₃)₂(en)]

(M = Pd, Pt) produces amphiphilic Pd and Pt complexes, [2][NO₃]₄ and [3][NO₃]₄. Complexes [2][NO₃]₄ and [3][NO₃]₄ form micelles in the presence of small amounts of dyes (Nile red and pyrene) in water. The critical micelle concentration (CMC) was determined by the absorption peak of the dye,

which is encapsulated in the micelles in solution. Micelle formation is confirmed by dynamic light scattering measurement of the solution and TEM (transmission electron microscopy) images of the micelles deposited from the solution. Addition of α -CD to the aqueous solution containing these amphiphilic complexes results in degradation of the micelle structure and the formation of [5]rotaxanes, [2(α -CD)₄][NO₃]₄ and [3(α -CD)₄][NO₃]₄.

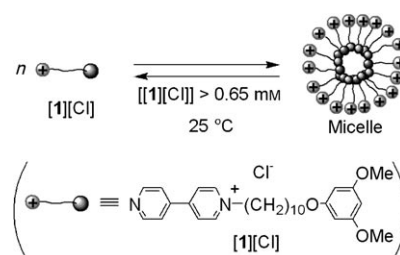
Keywords: amphiphiles • micelles • palladium • platinum • rotaxanes

Introduction

Amphiphilic compounds composed of a hydrophobic long alkyl chain and a hydrophilic functional group behave as surfactants that form aggregates, such as micelles and vesicles, in water.^[1] Transition-metal complexes having a cationic metal center and a ligand attached to the hydrophobic group also show an amphiphilic character.^[2] Dialkyl-2,2'-bipyridine-coordinated Ru complexes form normal micelles in water^[3] and inverted micelles in toluene.^[4] Aggregation of such metallosurfactants is flexible and is influenced by the temperature of the solution and by the new additive added to the solution. Addition of cyclodextrins (CDs) to the aqueous solution of micelles causes inclusion of the long alkyl chain of the amphiphilic compounds within the cavity of CD, forming pseudorotaxanes.^[5,6]

Recently, we prepared new amphiphilic compounds [4,4'-bpy-*N*-(CH₂)₁₀OC₆H₃-3,5-X₂][Cl] (X = OMe ([1][Cl]), *t*Bu), having an *N*-alkylbipyridinium and an oligomethylene group as the hydrophilic and hydrophobic groups, respectively.

They form micelles in aqueous solutions at concentrations higher than the critical micelle concentration (CMC, 0.65 mM of [1][Cl] at 25 °C; Scheme 1).^[7] Addition of α -CD to the solution converts the micelles into a pseudorotaxane of [1][Cl]. The molar ratio between [1] in the micelle and that in the pseudorotaxane is controlled reversibly by changing the temperature of the solution. A neutral Pt^{II} complex with analogous amphiphilic bipyridinium as the ligand, [(dmsol)PtCl₂{4,4'-bpy-*N*-(CH₂)₁₀OC₆H₃-3,5-*t*Bu₂}] [PtCl₃(dmsol)], forms [2]rotaxane with α -CD in the presence of DMSO. The reaction involves activation of the Pt–N bond caused by DMSO and inclusion of the liberated alkylbipyridinium by α -CD.^[8] Herein, we report the facile preparation of new amphiphilic palladium(II) and platinum(II) complexes containing *N*-alkylbipyridinium ligands and conversion of micellar



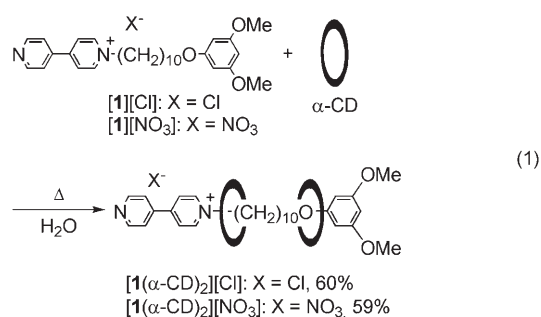
Scheme 1. Micelle formation of [4,4'-bpy-*N*-(CH₂)₁₀OC₆H₃-3,5-(OMe)₂][Cl] ([1][Cl]).

[a] T. Taira, Dr. Y. Suzaki, Prof. Dr. K. Osakada
Chemical Resources Laboratory
Tokyo Institute of Technology
4259 Nagatsuta, Midori-ku, Yokohama 226-8503 (Japan)
Fax: (+81)45-924-5224
E-mail: kosakada@res.titech.ac.jp

aggregates of the complexes to the rotaxanes with α -CDs. A part of this work has been reported in a preliminary form.^[9]

Results and Discussion

An *N*-alkylated bipyridinium compound **[1][Cl]** (or **[1][NO₃]**) forms a [3]pseudorotaxane with α -CD, as shown in Equation (1).



Heating an aqueous solution of α -CD and **[1][Cl]** at 60 °C for 0.5 h then cooling to 3 °C causes precipitation of **[1(α -CD)₂][Cl]** as a white solid from the solution (60% yield). A similar reaction using **[1][NO₃]**, obtained by anion exchange of **[1][Cl]** with AgNO₃, afforded **[1(α -CD)₂][NO₃]** in 59% yield. Figure 1 compares the ¹³C CP/MAS NMR spectra of α -CD, **[1(α -CD)₂][Cl]**, and **[1][Cl]**. Free α -CD shows small signals at δ = 81 and 98 arising from the C-4 and C-1 carbon atoms of the conformationally strained glycosidic linkage (Figure 1a).^[10] The absence of the corresponding signals in the spectrum of **[1(α -CD)₂][Cl]** (Figure 1b) suggests the symmetrically cyclic conformation of α -CD and release of the strain of the CD ring because of pseudorotaxane formation.^[11,12] The signals from the alkylbipyridinium in **[1(α -CD)₂][Cl]** are broadened more significantly than those of **[1**

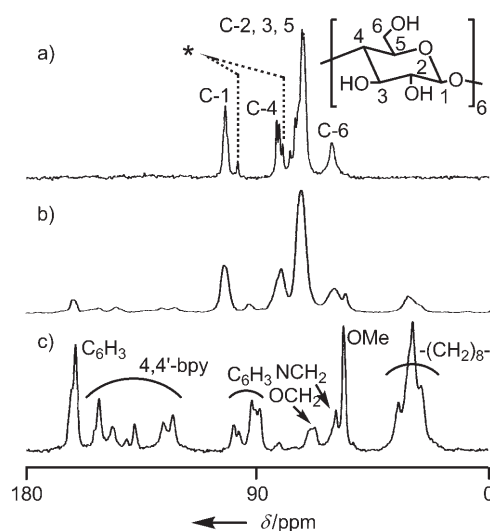


Figure 1. ¹³C CP/MAS NMR spectra (100 MHz, RT) of a) α -CD, b) **[1(α -CD)₂][Cl]**, and c) **[1][Cl]**. Peaks with an asterisk are assigned to C-1 and C-4 with a conformationally strained glycosidic linkage.

[Cl]. These results, as well as elemental analyses of **[1(α -CD)₂][Cl]** and **[1(α -CD)₂][NO₃]**, indicate formation of [3]pseudorotaxanes in the solid state. The X-ray powder diffraction pattern (XRD) of **[1(α -CD)₂][Cl]** differs from that of **[1][Cl]** and α -CD (Figure 2). The diffraction peak at 2θ =

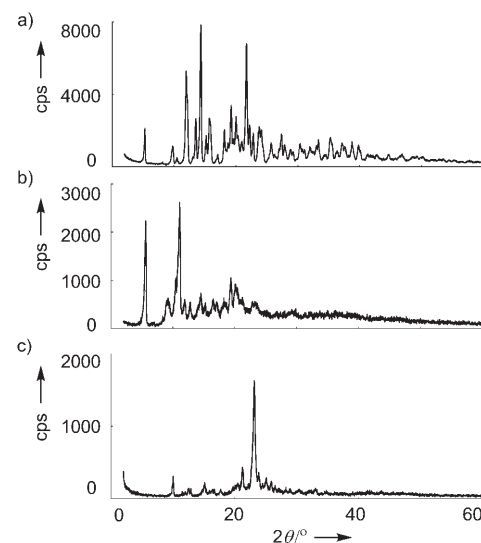


Figure 2. X-ray diffraction pattern of a) α -CD, b) **[1(α -CD)₂][Cl]**, and c) **[1][Cl]** (CuK α , RT).

11.1° (Figure 2b) is observed also in the XRD of the poly-pseudorotaxanes composed of β -CDs with poly(ϵ -caprolactone) and with poly(propylene glycol), and is characteristic of channel-type structures of CDs and their rotaxanes.^[13]

A D₂O solution of the [3]pseudorotaxane contains **[1(α -CD)][Cl]** and α -CD as the major species. The ¹³C{¹H} NMR spectrum of the solution, obtained by dissolution of **[1(α -CD)₂][Cl]** in D₂O, exhibits two sets of the signals of α -CD

Abstract in Japanese:

N-アルキルピピリジニウム誘導体[4,4'-bpy-*N*-(CH₂)₁₀OC₆H₃-3,5-(OMe)₂][X] (X = Cl, NO₃)と α -シクロデキストリン(α -CD)は水溶液中で[3]擬ロタキサンを生成した。[3]擬ロタキサンは二つの α -CDがアルキルピピリジニウムを包接した構造を有し、そのM(NO₃)₂(en) (M = Pd, Pt, en = 1,2-エチレンジアミン)との2:1の反応で、二つの[3]擬ロタキサンが窒素-金属配位結合によって連結された[5]ロタキサンが得られた。この[5]ロタキサンは、その軸状分子に相当するパラジウムあるいは白金錯体と α -CDとの直接反応によっても合成できる。この反応に用いたビス(ピピリジニウム)パラジウムおよび白金錯体は水溶液中でミセルを形成するので、上記の[5]ロタキサン形成反応の過程においては、両親媒性金属錯体が形成するミセル構造が、 α -CDとのロタキサン形成にともなって失われていることがわかった。この超分子の構造変換反応を紫外可視吸収スペクトルによって追跡した。

(Figure 3b). One is assigned to those of the inclusion complex $[1(\alpha\text{-CD})][\text{Cl}]$ ($\delta=62.1, 74.1, 74.5, 76.4, 83.7, 104.6$ ppm), and the other arises from free $\alpha\text{-CD}$ ($\delta=62.9$,

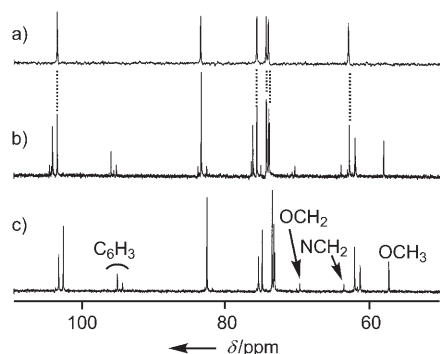


Figure 3. $^{13}\text{C}\{^1\text{H}\}$ NMR spectra of the D_2O solution obtained by dissolution of a) $\alpha\text{-CD}$, b) $[1(\alpha\text{-CD})_2][\text{Cl}]$, and c) $[3(\alpha\text{-CD})_4][\text{NO}_3]_4$ at room temperature (100 MHz). Sodium 3-(trimethylsilyl)-1-propanesulfonate (DSS) was used as an external standard.

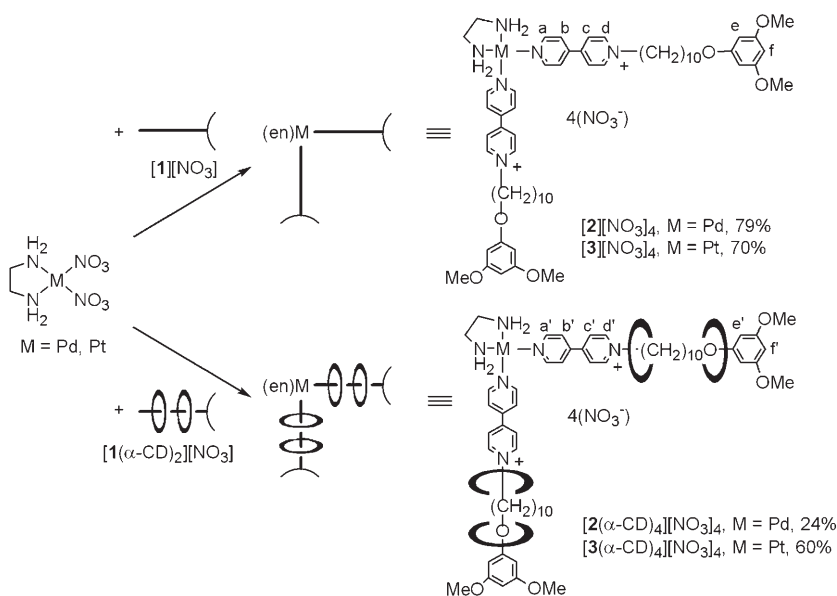
74.2, 74.5, 75.9, 83.7, 103.9 ppm). Signals of $[1][\text{Cl}]$ that should show peaks at $\delta=95.0, 95.9$ ppm were not observed. Small signals in Figure 3b ($\delta=63.1, 75.3, 76.7, 82.9, 84.2$ ppm) may be assigned to an isomer, such as [2]pseudorotaxane ($[1(\alpha\text{-CD})][\text{Cl}]$) with different orientations of $\alpha\text{-CD}$. The ^1H NMR peak positions of $[1(\alpha\text{-CD})][\text{Cl}]$ ($\delta=5.94, 6.04, 7.73, 8.22, 8.58, 8.80$ ppm) differ distinctly from the corresponding signals of $[1][\text{Cl}]$ ($\delta=5.47, 5.63, 7.62, 8.15, 8.53, 8.74$ ppm). The ^1H NMR spectrum in D_2O does not change significantly even at 80°C .

The formation of $[1(\alpha\text{-CD})][\text{Cl}]$ was confirmed by electrospray ionization mass spectrum (ESI-MS), which shows a peak arising from $[1(\alpha\text{-CD})]^+$ at m/z 1422. All these results indicate that $[1(\alpha\text{-CD})_2][\text{Cl}]$ keeps the [3]pseudorotaxane structure in the solid state and that dissolution of $[1(\alpha\text{-CD})_2][\text{Cl}]$ in D_2O yields an equilibrated mixture containing $\alpha\text{-CD}$ and $[1(\alpha\text{-CD})][\text{Cl}]$. The solution may contain [3]rotaxane $[1(\alpha\text{-CD})_2][\text{Cl}]$ as well.^{[6], [14]} Unfortunately, the spectroscopic data are not sufficient to distinguish between [3]- and [2]rotaxane and, hence, also the actual ratio between them. Dissolution of $[1(\alpha\text{-CD})_2][\text{NO}_3]$ in $[\text{D}_6]\text{DMSO}$ at room temperature gives a 1:2 mixture of $[1][\text{NO}_3]$ and $\alpha\text{-CD}$. A hydrophobic interaction between $\alpha\text{-CD}$ and the axle molecule stabilizes the interlocked structure of the [2]pseudorotaxane in aque-

ous solution, while the interaction becomes less significant in organic solvents such as $[\text{D}_6]\text{DMSO}$. The bulky 3,5-dimethoxyphenyl and ionic bipyridinium end groups of the axle molecule also kinetically stabilize the pseudorotaxane structure.^[15]

Reaction of $[1][\text{NO}_3]$ with $[\text{M}(\text{NO}_3)_2(\text{en})]$ ($\text{M}=\text{Pd}, \text{Pt}$) produces $[\text{M}\{4,4'\text{-bpy-}N\text{-(CH}_2\text{)}_{10}\text{OC}_6\text{H}_3\text{-3,5-(OMe)}_2\}_2(\text{en})][\text{NO}_3]_4$ ($[2][\text{NO}_3]_4$, $\text{M}=\text{Pd}$, 79%; $[3][\text{NO}_3]_4$, $\text{M}=\text{Pt}$, 70%), as shown in Scheme 2. $[1(\alpha\text{-CD})_2][\text{NO}_3]$ with a [3]pseudorotaxane structure also reacts with the Pd and Pt complexes to form transition-metal-containing [5]rotaxanes $[\text{M}\{(4,4'\text{-bpy-}N\text{-(CH}_2\text{)}_{10}\text{OC}_6\text{H}_3\text{-3,5-(OMe)}_2)(\alpha\text{-CD})_2\}_2(\text{en})][\text{NO}_3]_4$ ($\text{M}=\text{Pd}$, $[2(\alpha\text{-CD})_4][\text{NO}_3]_4$, 24%; $\text{M}=\text{Pt}$, $[3(\alpha\text{-CD})_4][\text{NO}_3]_4$, 60%).^[16] Figure 3c shows the $^{13}\text{C}\{^1\text{H}\}$ NMR spectrum of $[3(\alpha\text{-CD})_4][\text{NO}_3]_4$, which shows two sets of signals of $\alpha\text{-CD}$ ($\delta=61.4$ and $62.1; 73.4$ and $73.5; 73.7$ (2C); 75.1 , and $75.6; 82.9$ (2C); 103.1 and 103.7 ppm). The signal at $\delta=82.9$ ppm is observed at a different position from the corresponding signal of free $\alpha\text{-CD}$, and the liberation of $\alpha\text{-CD}$ from the rotaxane does not occur.

The [5]rotaxane $[2(\alpha\text{-CD})_4][\text{NO}_3]_4$ is also formed from the



Scheme 2. Synthesis of $[2][\text{NO}_3]_4$, $[3][\text{NO}_3]_4$, $[2(\alpha\text{-CD})_4][\text{NO}_3]_4$, and $[3(\alpha\text{-CD})_4][\text{NO}_3]_4$.

reaction of $[2][\text{NO}_3]_4$ with $\alpha\text{-CD}$ in D_2O as shown in Equation (2). Figure 4 shows the ^1H NMR spectra of $[2][\text{NO}_3]_4$ and of mixtures containing $[2][\text{NO}_3]_4$ and $\alpha\text{-CD}$ ($[2][\text{NO}_3]_4=10$ mM, $[\alpha\text{-CD}]=20$ mM and 40 mM). Quantitative formation of $[2(\alpha\text{-CD})_4][\text{NO}_3]_4$ was observed within 10 min after addition of $\alpha\text{-CD}$ (4 equiv) to the solution of $[2][\text{NO}_3]_4$ at room temperature. A similar reaction of $[3][\text{NO}_3]_4$ with $\alpha\text{-CD}$ at room temperature does not give $[3(\alpha\text{-CD})_4][\text{NO}_3]_4$ but a mixture of unreacted $[3][\text{NO}_3]_4$ and $\alpha\text{-CD}$. Heating the mixture at 60°C for 21 h yields $[3(\alpha\text{-CD})_4][\text{NO}_3]_4$. The Pt-N bond is less labile than the Pd-N bond, and the bipyridinium ligand of $[3][\text{NO}_3]_4$ does not undergo partial dissociation

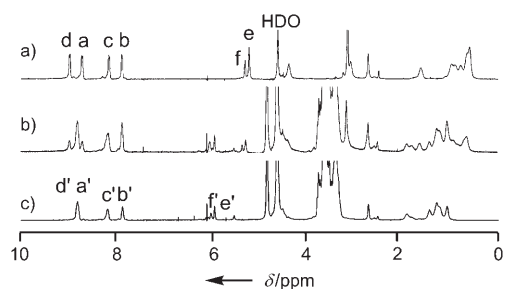
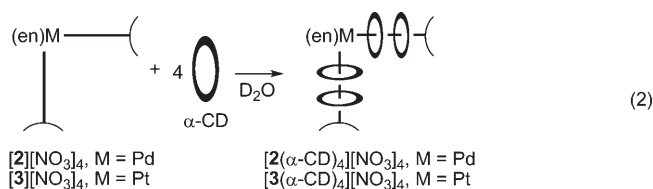


Figure 4. ¹H NMR spectra of a) [2][NO₃]₄ (10 mM), b) a mixture of [2][NO₃]₄ (10 mM) and α-CD (20 mM), and c) a mixture of [2][NO₃]₄ (10 mM) and α-CD (40 mM). For assignment of the signals, see Scheme 2.

at room temperature, although it is required for rotaxane formation via a “magic rod” procedure.^[8,17–19]

Micelle formation of the Pd and Pt complexes with amphiphilic ligands and their rotaxanes is examined by using



Nile red ($\lambda_{\text{max}} = 564 \text{ nm}$) as the hydrophobic pigments. Dissolution of [2][NO₃]₄ and Nile red ([Nile red] = 10 μM) in water leads to the aggregation of [2][NO₃]₄ to form micelles with encapsulated Nile red molecules in their core. Figure 5a shows the absorption spectra of the solutions with different concentrations of [2][NO₃]₄ (from 5 × 10⁻⁶ to 1.5 × 10⁻³ g mL⁻¹). The solutions with [2][NO₃]₄ below 6.3 × 10⁻⁴ g mL⁻¹ do not show any significant peak at 564 nm, but increasing the concentration above 1.3 × 10⁻³ g mL⁻¹ causes the appearance of a new absorption peak at the position assigned to the dye encapsulated within micelles. The CMC of [2][NO₃]₄ was determined to be 6.3 × 10⁻⁴ g mL⁻¹ (0.48 mM) at 25 °C on the basis of plots of absorbance at 564 nm versus

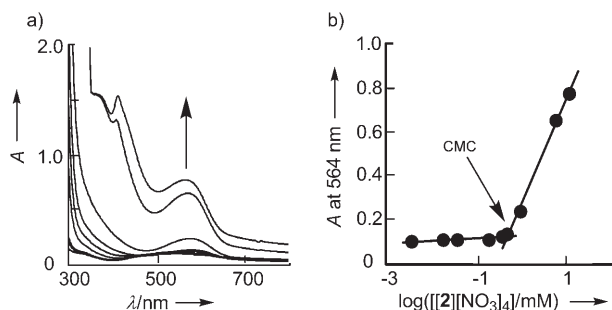


Figure 5. a) Absorption spectra of aqueous solutions of Nile red and [2][NO₃]₄ with various concentrations of [2][NO₃]₄ (from 5 × 10⁻⁶ to 1.5 × 10⁻³ g mL⁻¹). b) Plots of absorbance at 564 nm versus concentration of [2][NO₃]₄.

[2][NO₃]₄ (Figure 5b). The CMC of [3][NO₃]₄ was similarly determined to be 6.0 × 10⁻⁴ g mL⁻¹ (0.43 mM) at 25 °C. Dynamic light scattering (DLS) showed the average hydrodynamic radius of micelles in aqueous solution (10 mM, 21 °C) to be 16 nm for [2][NO₃]₄ and 5.9 nm for [3][NO₃]₄. Transmission electron microscope (TEM) images of [2][NO₃]₄ and [3][NO₃]₄ deposited from aqueous solution (1 mM) show the presence of spherical micelles (Figure 6), although the latter micelles aggregated to form larger particles during the sample preparation and measurement.

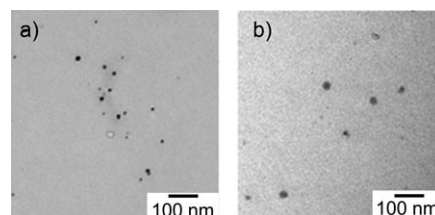


Figure 6. TEM images of the aggregates of a) [2][NO₃]₄ and b) [3][NO₃]₄.

Addition of α-CD to the micellar solution of [2][NO₃]₄ containing pyrene ([2][NO₃]₄] = 0.6 mM) at 25 °C decreased absorption at 341 nm (Figure 7a) depending on the amount of α-CD. Figure 7b shows a decrease of the absorbance at 341 nm from 0.65 to 0.41 caused by addition of α-CDs up to 4 equiv of the complex. Further addition of α-CD does not cause significant changes in the spectra.

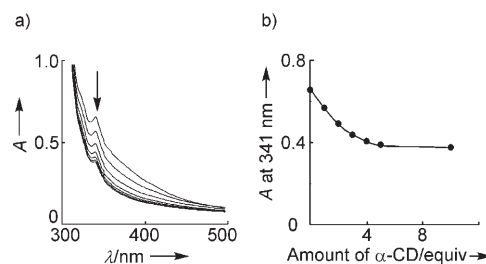
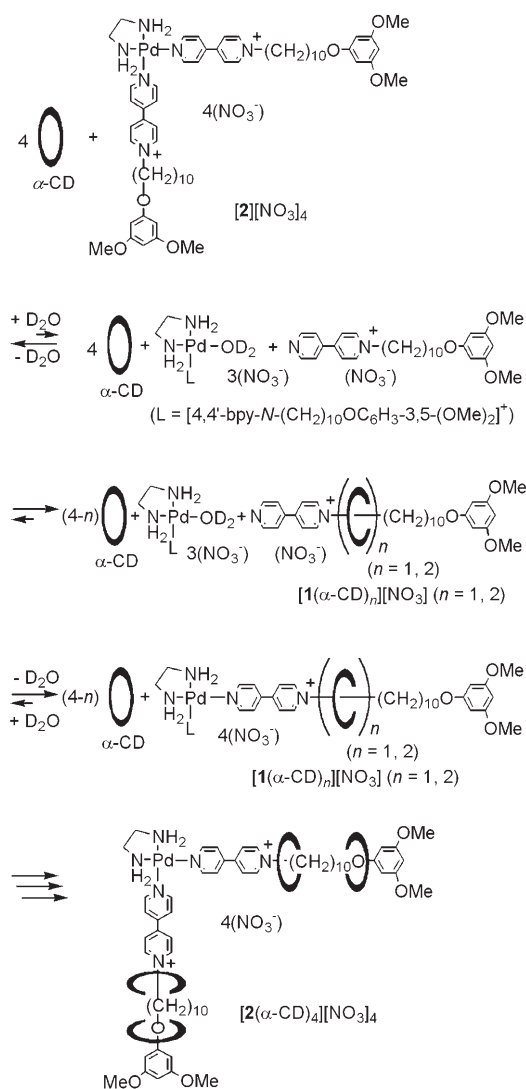


Figure 7. a) Absorption spectra of pyrene and [2][NO₃]₄ ([pyrene] = 10 μM, [2][NO₃]₄] = 0.6 mM) in aqueous solutions with various concentrations of α-CD (from 0 (0 equiv) to 6.0 mM (10 equiv)). b) Plots of absorbance at 341 nm versus amount of added α-CD.

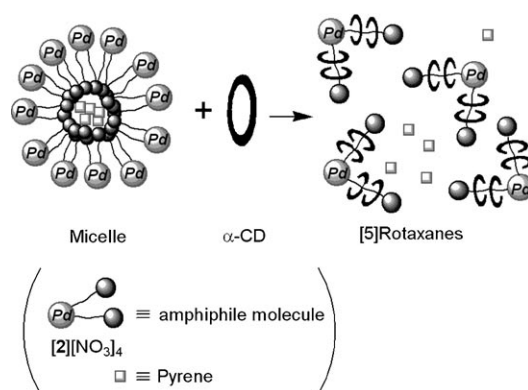
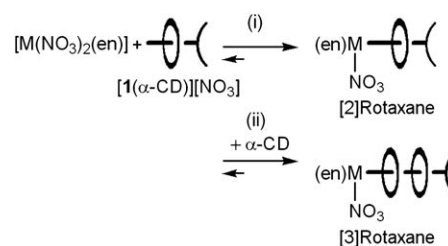
Scheme 3 depicts a plausible mechanism which accounts for [5]rotaxane formation from [2][NO₃]₄ and α-CD in D₂O (Figure 4). [2][NO₃]₄ is equilibrated with a mixture of [1][NO₃] and [Pd(L)(D₂O)(en)][NO₃]₃ (L = 4,4'-bpy-*N*-(CH₂)₁₀OC₆H₃-3,5-(OMe)₂) via partial dissociation of the bipyridinium ligand and its recoordination, while the equilibrium is favored to [2][NO₃]₄. Once liberated, [1][NO₃] and α-CD produce pseudorotaxanes [1(α-CD)_{*n*}][NO₃] (*n* = 1, 2), which are end-capped by [Pd(L)(D₂O)(en)][NO₃]₃ to form the [*n* + 1]rotaxane. Repetitive dissociation and formation of the metal–N bond accompanied by complexation with α-CD leads to the [5]rotaxane. Each step in the reaction is ap-

Scheme 3. Proposed mechanism for the formation of $[2(\alpha\text{-CD})_4][\text{NO}_3]_4$.

parently reversible, although high stability of the [5]rotaxane structure arises from the hydrophobic interaction between the cavity of $\alpha\text{-CD}$ and alkylbipyridinium ligands, making the reaction formally irreversible in D_2O . Heating of the solution (60°C) is required for the reaction of $[3][\text{NO}_3]_4$ with $\alpha\text{-CD}$ to activate the Pt–N bond, which is stronger than the Pd–N bond.^[8,20]

The amphiphilic molecule $[2][\text{NO}_3]_4$ at concentrations above CMC forms micelles in water via encapsulation of the dye. Addition of $\alpha\text{-CD}$ to the solution reorganizes the aggregates to form the rotaxanes with $\alpha\text{-CD}$, as summarized in Scheme 4. The incorporated dye was released by degradation of the micelles because the rotaxanes could not form micelles that can solubilize the dye in water.

Formation of the [5]rotaxane from $[\text{M}(\text{NO}_3)_2(\text{en})]$ and $[\mathbf{1}(\alpha\text{-CD})_2][\text{NO}_3]$ may involve the reactions in Scheme 5 because $[\mathbf{1}(\alpha\text{-CD})_2][\text{NO}_3]$ exists as a mixture of $[\mathbf{1}(\alpha\text{-CD})_2]$

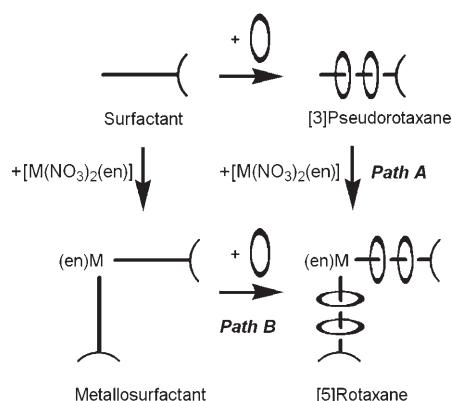
Scheme 4. Proposed mechanism of changes in absorption spectrum of a solution of pyrene and $[2][\text{NO}_3]_4$ by addition of $\alpha\text{-CD}$.

Scheme 5. Pathway for [3]rotaxane formation.

$[\text{NO}_3]$, $[\mathbf{1}(\alpha\text{-CD})][\text{NO}_3]$, and $\alpha\text{-CD}$ in aqueous solution. Initially formed $[\mathbf{1}(\alpha\text{-CD})][\text{NO}_3]$ coordinates to the metal center to yield [2]rotaxane (Scheme 5 (i)), which is followed by incorporation of an additional $\alpha\text{-CD}$ induced by dissociation of the alkylbipyridinium ligand (Scheme 5 (ii)). The latter reaction takes place smoothly, similarly to the reactions shown in Scheme 3.

Conclusions

In this paper, we have described the synthesis of [5]rotaxanes composed of four $\alpha\text{-CD}$ s and bis(bipyridinium)palladium and platinum complexes as the macrocyclic and the axle components, respectively. The [5]rotaxanes have been prepared by reactions of [3]pseudorotaxanes with $[\text{M}(\text{NO}_3)_2(\text{en})]$ (Scheme 6, Path A) and of $\alpha\text{-CD}$ with the amphiphilic complex (Scheme 6, Path B). Amphiphilic bis(bipyridinium)complexes, which are double-tailed surfactants, form micelles in water above their CMC. Addition of $\alpha\text{-CD}$ to the micellar solution causes degradation of the micelle and affords [5]rotaxanes of the individual molecules of the complexes. This transformation of metallomicelles (higher-order supramolecules) into rotaxanes (lower-order supramolecules) may provide a new method to control aggregation and functions of the metallosurfactants.



Scheme 6. Pathway for the synthesis of metallosurfactant, [3]pseudorotaxane, and [5]rotaxane.

Experimental Section

Materials and Methods

[M(NO₃)₂(en)] (M = Pd, Pt) were prepared according to the literature method.^[21,22] The other chemicals were commercially available and used without further purification. ¹H and ¹³C[¹H] NMR spectra were recorded on Varian MERCURY300 and JEOL EX-400 spectrometers. 3-(Trimethylsilyl)-1-propanesulfonic acid, sodium salt (DSS) was used as an external standard in the ¹³C[¹H] NMR measurements in D₂O. IR absorption spectra were recorded on Shimadzu FT/IR-8100 spectrometers. Elemental analyses were carried out with a Yanaco MT-5 CHN autorecorder. The absorption spectra were recorded using a JASCO V-530 UV/Vis spectrometer. A 10 μL aliquot of a 2.0 μM solution of Nile red in DMSO was transferred to 2.0 cm³ of each sample. Before measuring, the samples were stored at adequate temperature using a JASCO EHC-477 peltiere-type thermostated cell holder. The aggregates of the sample were observed by transmission electron microscopy (TEM, HITACHI 7000) operating at 100 kV. The hydrodynamic size of the micelles in aqueous solution was measured using an Otsuka Electronics Co., Ltd. DLS-7000 spectrophotometer equipped with a 10 mW He-Ne laser operating at 632.8 nm. Measurement was performed at an angle of 90°, and the data obtained were fitted using the CONTIN algorithm. Electrospray ionization mass spectrometry (ESI-MS) was recorded on a ThermoQuest Finnigan LCQ Duo mass spectrometer.

Synthesis

[4,4'-bpy-*N*-(CH₂)₁₀OC₆H₃-3,5-(OMe)₂][Cl] ([I][Cl]): [I][Cl] was prepared according to the literature method.^[7] ¹³C[¹H] NMR (100 MHz, D₂O, RT): δ = 28.3 (CH₂), 28.4 (CH₂), 31.4 (CH₂), 31.5 (CH₂), 31.7 (CH₂), 31.7 (CH₂), 31.8 (CH₂), 33.5 (CH₂), 57.6 (OCH₃), 64.3 (NCH₂), 70.4 (OCH₂), 95.0 (C₆H₃), 95.9 (C₆H₃), 124.8 (C₁₀H₈N₂), 128.3 (C₁₀H₈N₂), 144.2 (C₁₀H₈N₂), 147.4 (C₁₀H₈N₂), 152.8 (C₁₀H₈N₂), 155.8 (C₁₀H₈N₂), 163.1 (C₆H₃), 163.7 ppm (C₆H₃).

[4,4'-bpy-*N*-(CH₂)₁₀OC₆H₃-3,5-(OMe)₂][NO₃] ([I][NO₃]): AgNO₃ (170 mg, 1.0 mmol) was added to an aqueous solution (10 mL) containing [4,4'-bpy-*N*-(CH₂)₁₀OC₆H₃-3,5-(OMe)₂][Cl] ([I][Cl]) (500 mg, 1.0 mmol), and the mixture was stirred for 10 h at room temperature in the dark. The formed solid was collected by filtration and the product was extracted with acetone (20 mL). Evaporation of the solvent and drying under reduced pressure yielded [I][NO₃] as a brown solid (392 mg, 0.77 mmol, 77%). IR (KBr disk, RT): $\tilde{\nu}$ = 1385 cm⁻¹; ¹H NMR (400 MHz, [D₆]DMSO, RT): δ = 1.22–1.41 (12H; CH₂), 1.65 (t, ³J_{H,H} = 7 Hz, 2H; OCH₂CH₂), 1.94 (br, 2H; NCH₂CH₂), 3.68 (s, 6H; OCH₃), 3.87 (t, ³J_{H,H} = 7 Hz, 2H; OCH₂), 4.62 (t, ³J_{H,H} = 7 Hz, 2H; NCH₂), 6.04 (3H; C₆H₃), 8.03 (d, ³J_{H,H} = 6 Hz, 2H; C₁₀H₈N₂), 8.62 (d, ³J_{H,H} = 7 Hz, 2H; C₁₀H₈N₂), 8.85 (d, ³J_{H,H} = 6 Hz, 2H; C₁₀H₈N₂), 9.22 ppm (d, ³J_{H,H} = 6 Hz, 2H; C₁₀H₈N₂); ¹³C[¹H] NMR (100 MHz, [D₆]DMSO, RT): δ = 25.4 (CH₂), 25.5 (CH₂), 28.4 (CH₂), 28.7 (3C, CH₂), 28.9 (CH₂), 30.7 (CH₂), 55.1

(OCH₃), 60.4 (NCH₂), 67.3 (OCH₂), 92.7 (C₆H₃), 93.1 (C₆H₃), 121.8 (C₁₀H₈N₂), 125.3 (C₁₀H₈N₂), 140.7 (C₁₀H₈N₂), 145.2 (C₁₀H₈N₂), 150.8 (C₁₀H₈N₂), 152.1 (C₁₀H₈N₂), 160.4 (C₆H₃), 161.0 ppm (C₆H₃); elemental analysis calcd (%) for C₂₈H₃₇N₃O₆(H₂O) (529.6): C 63.50, H 7.42, N 7.93; found: C 63.78, H 7.03, N 7.91.

[[4,4'-bpy-*N*-(CH₂)₁₀OC₆H₃-3,5-(OMe)₂](α-CD)₂][Cl] ([I(α-CD)₂][Cl]): [4,4'-bpy-*N*-(CH₂)₁₀OC₆H₃-3,5-(OMe)₂][Cl] ([I][Cl]) (478 mg, 0.99 mmol) was dissolved in H₂O (10 mL) containing α-CD (1.95 g, 2.0 mmol). The mixture was stirred for 0.5 h at 60 °C and kept for 18 h at 3 °C. The solid separated from the solution was collected by filtration, washed with water, and dried under reduced pressure to give [I(α-CD)₂][Cl] (1.43 g, 0.59 mmol, 60%). IR (KBr disk, RT): $\tilde{\nu}$ = 3000–3700 (OH), 1206 cm⁻¹ (C–O–C); elemental analysis calcd (%) for C₁₀₀H₁₅₇N₂O₆₃Cl·6(H₂O) (2538.9): C 47.31, H 6.71, N 1.10, Cl 1.40; found: C 47.25, H 6.59, N 1.23, Cl 1.31. The following data are assigned to [I(α-CD)₂][Cl]. Details are shown in the text. ¹H NMR (300 MHz, D₂O, RT): δ = 1.02–1.59 (14H; CH₂-axle), 1.70–2.04 (br, 2H; NCH₂CH₂), 3.29–3.82 (m, 80H; CH-α-CD, CH₂-α-CD, OCH₂-axle, OMe), 4.86 (s, 12H; CH-α-CD), 5.94 (s, 2H; ortho-C₆H₃), 6.04 (s, 1H; para-C₆H₃), 7.73 (br, 2H; C₁₀H₈N₂), 8.22 (d, ³J_{H,H} = 5 Hz, 2H; C₁₀H₈N₂), 8.58 (br, 2H; C₁₀H₈N₂), 8.80 ppm (d, ³J_{H,H} = 5 Hz, 2H; C₁₀H₈N₂). The signal of the NCH₂ hydrogen atoms overlapped with the signal of HDO (δ = 4.63 ppm). ¹³C[¹H] NMR (300 MHz, D₂O, RT): δ = 28.7 (CH₂), 29.6 (CH₂), 31.8 (CH₂), 32.3 (CH₂), 32.7 (CH₂), 33.4 (CH₂), 33.5 (CH₂), 33.6 (CH₂), 58.1 (OMe), 62.1 (α-CD), 64.1 (NCH₂), 70.6 (OCH₂), 74.1 (α-CD), 74.5 (α-CD), 76.4 (α-CD), 83.7 (α-CD), 95.6 (C₆H₃), 96.4 (C₆H₃), 104.6 (α-CD), 125.0 (C₁₀H₈N₂), 128.6 (C₁₀H₈N₂), 145.1 (C₁₀H₈N₂), 147.1 (C₁₀H₈N₂), 152.4 (C₁₀H₈N₂), 156.2 (C₁₀H₈N₂), 162.4 (C₆H₃), 163.7 ppm (C₆H₃); MS (ESI) calcd (%) for C₆₄H₉₇N₂O₃₃⁺: found: *m/z* = 1422 [M–Cl]⁺.

[[4,4'-bpy-*N*-(CH₂)₁₀OC₆H₃-3,5-(OMe)₂](α-CD)₂][NO₃] ([I(α-CD)₂][NO₃]): [4,4'-bpy-*N*-(CH₂)₁₀OC₆H₃-3,5-(OMe)₂][NO₃] ([I][NO₃]) (1.5 g, 2.9 mmol) was dissolved in H₂O (45 mL) containing α-CD (5.8 g, 6.0 mmol). The mixture was stirred for 0.5 h at 70 °C and kept for 17 h at room temperature. The formed precipitation was collected by filtration, washed with water, and dried under reduced pressure to give [I(α-CD)₂][NO₃] (4.2 g, 1.7 mmol, 59%). IR (KBr disk, RT): $\tilde{\nu}$ = 1385 cm⁻¹; elemental analysis calcd (%) for C₁₀₀H₁₅₇N₃O₆₆·6(H₂O) (2565.4): C 46.82, H 6.64, N 1.64; found: C 46.69, H 6.27, N 1.62.

[Pd{4,4'-bpy-*N*-(CH₂)₁₀OC₆H₃-3,5-(OMe)₂}(en)][NO₃]₄ ([2][NO₃]₄): An aqueous solution (20 mL) containing [Pd(NO₃)₂(en)] (42 mg, 0.14 mmol) and [I][NO₃] (150 mg, 0.29 mmol) was stirred in the dark for 1 h at room temperature and the resulting precipitate was removed by filtration. Evaporation of the solvent gave the product, which was dried under reduced pressure to yield [2][NO₃]₄ (139 mg, 0.11 mmol, 79%). IR (KBr disk, RT): $\tilde{\nu}$ = 1385 cm⁻¹; ¹H NMR (400 MHz, D₂O, RT): δ = 0.62–1.20 (28H; CH₂), 1.70 (br, 4H; NCH₂CH₂), 2.82 (s, 4H; en), 3.22 (16H; OCH₃, OCH₂), 4.44 (br, 4H; NCH₂), 5.39 (s, 4H; ortho-C₆H₃), 5.43 (s, 2H; para-C₆H₃), 7.94 (br, 4H; C₁₀H₃N₂), 8.23 (br, 4H; C₁₀H₃N₂), 8.77 (br, 4H; C₁₀H₃N₂), 9.00 ppm (br, 4H; C₁₀H₃N₂); ¹³C[¹H] NMR (100 MHz, D₂O, RT): δ = 27.7 (2C; CH₂), 30.8 (2C; CH₂), 31.0 (2C; CH₂), 31.2 (CH₂), 32.9 (CH₂), 48.8 (en), 56.6 (OCH₃), 63.6 (NCH₂), 69.4 (OCH₂), 93.8 (para-C₆H₃), 94.8 (ortho-C₆H₃), 126.6 (C₁₀H₃N₂), 127.6 (C₁₀H₃N₂), 146.4 (C₁₀H₃N₂), 146.5 (C₁₀H₃N₂), 152.5 (C₁₀H₃N₂), 154.0 (C₁₀H₃N₂), 161.9 (meta-C₆H₃), 162.4 ppm (ipso-C₆H₃); elemental analysis calcd (%) for C₅₈H₈₂N₁₀O₁₈Pd·3(H₂O) (1367.8): C 50.93, H 6.48, N 10.24; found: C 50.70, H 6.32, N 10.10.

[Pt{4,4'-bpy-*N*-(CH₂)₁₀OC₆H₃-3,5-(OMe)₂}(en)][NO₃]₄ ([3][NO₃]₄): An aqueous solution (30 mL) containing [Pt(NO₃)₂(en)] (38 mg, 0.10 mmol) and [I][NO₃] (100 mg, 0.20 mmol) was stirred in the dark for 18 h at 60 °C and the resulting precipitate was removed by filtration. Evaporation of the solvent gave the product, which was dried under reduced pressure to yield [3][NO₃]₄ (98 mg, 0.070 mmol, 70%). ¹H NMR (300 MHz, D₂O, RT): δ = 0.61–1.16 (28H; CH₂), 1.67 (br, 4H; NCH₂CH₂), 2.67 (br, 4H; en), 3.09 (br, 4H; OCH₃), 3.27 (s, 12H; OCH₃), 4.41 (br, 4H; NCH₂), 5.18 (s, 4H; ortho-C₆H₃), 5.35 (s, 2H; para-C₆H₃), 7.85 (d, ³J_{H,H} = 5 Hz, 4H; C₁₀H₈N₂), 8.14 (d, ³J_{H,H} = 5 Hz, 4H; C₁₀H₈N₂), 8.71 (d, 4H, C₁₀H₈N₂, ³J_{H,H} = 6 Hz), 9.00 ppm (d, ³J_{H,H} = 6 Hz, 4H; C₁₀H₈N₂); ¹³C[¹H] NMR (100 MHz, D₂O, RT): δ = 27.6 (2C; CH₂), 30.8 (2C; CH₂),

30.9 (CH₂), 31.0 (CH₂), 31.2 (CH₂), 32.9 (CH₂), 49.5 (en), 56.6 (OCH₃), 63.7 (NCH₂), 69.3 (OCH₂), 93.8 (*para*-C₆H₃), 94.7 (*ortho*-C₆H₃), 127.0 (C₁₀H₈N₂), 127.5 (C₁₀H₈N₂), 146.0 (C₁₀H₈N₂), 146.5 (C₁₀H₈N₂), 152.2 (C₁₀H₈N₂), 154.8 (C₁₀H₈N₂), 161.8 (*meta*-C₆H₃), 162.3 ppm (*ipso*-C₆H₃); elemental analysis calcd (%) for C₃₈H₃₂N₁₀O₁₈Pt·3(H₂O) (1456.5): C 47.83, H 6.09, N 9.62; found: C 47.57, H 5.78, N 9.62.

[Pd{(4,4'-bpy-*N*-(CH₂)₁₀OC₆H₃-3,5-(OMe)₂)(α-CD)₂(en)}][NO₃]₄ ([2(α-CD)₄][NO₃]₄): [1(α-CD)₂][Cl] (800 mg, 0.33 mmol) was dissolved in H₂O (30 mL) containing AgNO₃ (56 mg, 0.33 mmol). The mixture was stirred in the dark for 6 h at room temperature and the resulting precipitate was removed by filtration. [Pd(NO₃)₂(en)] (48 mg, 0.17 mmol) was added to the filtrate. The mixture was stirred for 1 h and then kept without stirring for 12 h at room temperature. Evaporation of the solvent gave the crude product, which was dissolved in water (20 mL), and the solution was treated by activated charcoal, filtrated, evaporated, and dried under reduced pressure to yield [2(α-CD)₄][NO₃]₄ (206 mg, 0.040 mmol, 24%). ¹H NMR (400 MHz, D₂O, RT): δ = 1.07–1.53 (28H; CH₂-axle), 1.96 (br, 4H; NCH₂CH₂), 2.77 (s, 4H; CH₂NH₂), 3.34–3.85 (160H; CH-α-CD, CH₂-α-CD, OCH₂-axle, OCH₃), 4.52 (br, NCH₂; 4H), 4.88 (br, 24H; CH-α-CD), 5.98 (s, 4H; *ortho*-C₆H₃), 6.08 (s, 2H; *para*-C₆H₃), 7.91 (br, 4H; C₁₀H₈N₂), 8.21 (br, 4H; C₁₀H₈N₂), 8.85 ppm (8H; C₁₀H₈N₂). Signals of the OH and NH₂ hydrogen atoms were not observed. ¹³C{¹H} NMR (100 MHz, D₂O, RT): δ = 28.1 (CH₂), 29.0 (CH₂), 31.2 (CH₂), 31.7 (CH₂), 32.0 (CH₂), 32.8 (2C; CH₂), 33.0 (CH₂), 48.7 (en), 57.4 (OCH₃), 61.4 (CH₂-α-CD), 62.2 (CH₂-α-CD), 63.6 (NCH₂), 69.8 (OCH₂), 73.4 (CH-α-CD), 73.5 (CH-α-CD), 73.7 (2C; CH-α-CD), 75.1 (CH-α-CD), 75.7 (CH-α-CD), 82.9 (2C; CH-α-CD), 94.8 (C₆H₃), 95.6 (C₆H₃), 103.7 (CH-α-CD), 103.9 (CH-α-CD), 126.8 (C₁₀H₈N₂), 128.0 (C₁₀H₈N₂), 146.4 (C₁₀H₈N₂), 147.2 (C₁₀H₈N₂), 153.7 (C₁₀H₈N₂), 161.4 (C₁₀H₈N₂), 162.7 (C₆H₃), 163.0 ppm (C₆H₃); elemental analysis calcd (%) for C₂₀₂H₃₂₂N₁₀O₁₃₈Pd·16(H₂O) (5493.4): C 44.17, H 6.50, N 2.55; found: C 44.17, H 6.30, N 2.19.

[Pt{(4,4'-bpy-*N*-(CH₂)₁₀OC₆H₃-3,5-(OMe)₂)(α-CD)₂(en)}][NO₃]₄ ([3(α-CD)₄][NO₃]₄): [1(α-CD)₂][Cl] (100 mg, 0.041 mmol) was dissolved in H₂O (5.0 mL) containing AgNO₃ (6.8 mg, 0.040 mmol). The mixture was stirred in the dark for 6 h at room temperature and the resulting precipitate was removed by filtration. [Pt(NO₃)₂(en)] (7.6 mg, 0.020 mmol) was added to the filtrate and stirred for 15 h at 60 °C. The resulting solids were removed by filtration and evaporation of the solvent gave the crude product, which was dissolved in water (20 mL) and treated by activated charcoal, filtrated, evaporated, and dried under reduced pressure to yield [3(α-CD)₄][NO₃]₄ (65 mg, 0.012 mmol, 60%). ¹H NMR (300 MHz, D₂O, RT): δ = 1.22–1.41 (24H; CH₂-axle), 1.49 (br, 4H; OCH₂CH₂), 1.95 (br, 4H; NCH₂CH₂), 2.69 (s, 4H; CH₂NH₂), 3.28–3.86 (160H; CH-α-CD, CH₂-α-CD, OCH₂-axle, OCH₃), 4.88 (d, ³J_{H,H} = 5 Hz, 24H; CH-α-CD), 5.98 (s, 4H; *ortho*-C₆H₃), 6.10 (s, 2H; *para*-C₆H₃), 7.90 (d, ³J_{H,H} = 5 Hz, 4H; C₁₀H₈N₂), 8.24 (d, ³J_{H,H} = 7 Hz, 4H; C₁₀H₈N₂), 8.87 ppm (8H; C₁₀H₈N₂). The signal of the NCH₂ hydrogen atoms overlapped with the signal of H₂O (δ = 4.63 ppm). Signals of the OH and NH₂ hydrogen atoms were not observed. ¹³C{¹H} NMR (100 MHz, D₂O, RT): δ = 28.1 (CH₂), 29.1 (CH₂), 31.2 (CH₂), 31.7 (CH₂), 32.1 (CH₂), 32.8 (CH₂), 32.9 (CH₂), 33.0 (CH₂), 49.4 (en), 57.3 (OCH₃), 61.4 (CH₂-α-CD), 62.1 (CH₂-α-CD), 63.6 (NCH₂), 69.9 (OCH₂), 73.4 (CH-α-CD), 73.5 (CH-α-CD), 73.7 (2C; CH-α-CD), 75.1 (CH-α-CD), 75.6 (CH-α-CD), 82.9 (2C; CH-α-CD), 94.8 (C₆H₃), 95.5 (C₆H₃), 103.1 (CH-α-CD), 103.7 (CH-α-CD), 127.2 (C₁₀H₈N₂), 128.0 (C₁₀H₈N₂), 146.5 (C₁₀H₈N₂), 147.0 (C₁₀H₈N₂), 152.7 (C₁₀H₈N₂), 154.5 (C₁₀H₈N₂), 161.5 (C₆H₃), 162.7 ppm (C₆H₃).

Acknowledgements

We thank our colleagues in the Chemical Resources Laboratory of Tokyo Institute of Technology for their technical support and discussions; Prof. Takakazu Yamamoto for dynamic light scattering (DLS) measurements, Prof. Tomokazu Iyoda and Dr. Kaori Kamata for TEM measurements, Prof. Munetaka Akita for ESI-MS measurements, and Dr. Yoshiyuki Nakamura for the ¹³C CP/MAS NMR measurements. This work was supported by Grant-in-Aid for Scientific Research for Young Scien-

tists from the Ministry of Education, Culture, Sports, Science and Technology, Japan (19750044), and by the Global COE Program "Education and Research Center for Emergence of New Molecular Chemistry".

- a) M. N. Jones, D. Chapman, *Micelles, Monolayers, and Biomembranes*, Wiley-Liss, New York, **1995**; b) C. Tanford, *The Hydrophobic Effect*, Wiley, New York, **1973**.
- a) B. Donnio, *Curr. Opin. Colloid Interface Sci.* **2002**, *7*, 371; b) P. C. Griffiths, I. A. Fallis, T. Chuenpratoom, R. Wataneski, *Adv. Colloid Interface Sci.* **2006**, *122*, 107.
- a) J. Bowers, M. J. Danks, D. W. Bruce, R. K. Heenan, *Langmuir* **2003**, *19*, 292; b) J. Bowers, M. J. Danks, D. W. Bruce, J. R. P. Webster, *Langmuir* **2003**, *19*, 299; c) J. Bowers, K. E. Amos, D. W. Bruce, J. R. P. Webster, *Langmuir* **2005**, *21*, 1346.
- D. Domínguez-Gutiérrez, M. Surtchev, E. Eiser, C. J. Elsevier, *Nano Lett.* **2006**, *6*, 145.
- a) *Molecular Catenanes, Rotaxanes and Knots* (Eds.: J.-P. Sauvage, C. Dietrich-Buchecker), Wiley-VCH, Weinheim, **1999**; b) J. Szejtli, *Topics in Inclusion Science: Cyclodextrin Technology*, Kluwer, Boston, **1988**; c) A. Harada, *Acc. Chem. Res.* **2001**, *34*, 456; d) G. Wenz, B.-H. Han, A. Müller, *Chem. Rev.* **2006**, *106*, 782.
- a) T. Okubo, H. Kitano, N. Ise, *J. Phys. Chem.* **1976**, *80*, 2661; b) R. Palepu, V. C. Reinsborough, *Can. J. Chem.* **1988**, *66*, 325; c) M. Tunçay, S. D. Christian, *J. Colloid Interface Sci.* **1994**, *167*, 181; d) H. Mwakibete, R. Cristantino, D. M. Bloor, E. Wyn-Jones, J. F. Holzwarth, *Langmuir* **1995**, *11*, 57; e) R. Guo, X. J. Zhu, X. Guo, *Colloid Polym. Sci.* **2003**, *281*, 876; f) N. Funasaki, S. Ishikawa, S. Neya, *J. Phys. Chem. B* **2004**, *108*, 9593; g) A. A. Rafati, A. Bagheri, *Bull. Chem. Soc. Jpn.* **2004**, *77*, 485; h) P. Sehgal, M. Sharma, R. Wimmer, K. L. Larsen, D. E. Otzen, *Colloid Polym. Sci.* **2006**, *284*, 916; i) A. Diaz, P. A. Quintela, J. M. Schuette, A. E. Kaifer, *J. Phys. Chem.* **1988**, *92*, 3537; j) P. Choppinet, L. Jullien, B. Valeur, *J. Chem. Soc. Perkin Trans. 2* **1999**, 249; k) G. M. Nicolle, A. E. Merbach, *Chem. Commun.* **2004**, 854.
- Y. Suzaki, T. Taira, D. Takeuchi, K. Osakada, *Org. Lett.* **2007**, *9*, 887.
- a) Y. Suzaki, T. Taira, K. Osakada, *Dalton Trans.* **2006**, 5345; b) Y. Suzaki, T. Taira, K. Osakada, *Transition Met. Chem.* **2007**, *32*, 753.
- T. Taira, Y. Suzaki, K. Osakada, *Chem. Lett.* **2008**, 182.
- a) P. C. Manor, W. Saenger, *J. Am. Chem. Soc.* **1974**, *96*, 3630; b) M. J. Gidley, S. M. Bociek, *J. Am. Chem. Soc.* **1988**, *110*, 3820.
- a) A. Harada, M. Kamachi, *Macromolecules* **1990**, *23*, 2821; b) A. Harada, J. Li, M. Kamachi, *Macromolecules* **1993**, *26*, 5698.
- I. Yamaguchi, H. Ishii, K. Osakada, T. Yamamoto, S. Fukuzawa, *Bull. Chem. Soc. Jpn.* **1999**, *72*, 1541.
- M. Osaki, Y. Takashima, H. Yamaguchi, A. Harada, *J. Am. Chem. Soc.* **2007**, *129*, 14452.
- Examples of 1:2 complexes of surfactant and α-CD: a) W. M. Z. Wan Yunus, J. Taylor, D. M. Bloor, D. G. Hall, E. Wyn-Jones, *J. Phys. Chem.* **1992**, *96*, 8979; b) N. Funasaki, S. Ishikawa, S. Neya, *Langmuir* **2000**, *16*, 5584; c) N. Funasaki, H. Yodo, S. Hada, S. Neya, *Bull. Chem. Soc. Jpn.* **1992**, *65*, 1323; d) N. Funasaki, M. Ohigashi, S. Hada, S. Neya, *Langmuir* **2000**, *16*, 383.
- a) Y. Kawaguchi, A. Harada, *J. Am. Chem. Soc.* **2000**, *122*, 3797; b) T. Oshikiri, Y. Takashima, H. Yamaguchi, A. Harada, *J. Am. Chem. Soc.* **2005**, *127*, 12186.
- Examples of [5]rotaxanes: a) N. Solladié, J.-C. Chambron, C. O. Dietrich-Buchecker, J.-P. Sauvage, *Angew. Chem.* **1996**, *108*, 957; *Angew. Chem. Int. Ed. Engl.* **1996**, *35*, 906; b) N. Solladié, J.-C. Chambron, J.-P. Sauvage, *J. Am. Chem. Soc.* **1999**, *121*, 3684; c) D. Tuncel, N. Cindir, Ü. Koldemir, *J. Inclusion Phenom. Macrocyclic Chem.* **2006**, *55*, 373; d) S.-G. Roh, K.-M. Park, G.-J. Park, S. Sakamoto, K. Yamaguchi, K. Kim, *Angew. Chem.* **1999**, *111*, 671; *Angew. Chem. Int. Ed.* **1999**, *38*, 637; e) N. Watanabe, T. Yagi, N. Kihara, T. Takata, *Chem. Commun.* **2002**, 2720.
- J. S. Hannam, T. J. Kidd, D. A. Leigh, A. J. Wilson, *Org. Lett.* **2003**, *5*, 1907.
- Y. Furusho, T. Hasegawa, A. Tsuboi, N. Kihara, T. Takata, *Chem. Lett.* **2000**, 18.

- [19] Y. Suzaki, K. Osakada, *Chem. Asian J.* **2006**, *1*, 331.
- [20] a) R. S. Wylie, D. H. Macartney, *J. Am. Chem. Soc.* **1992**, *114*, 3136;
b) R. S. Wylie, D. H. Macartney, *Supramol. Chem.* **1993**, *3*, 29;
c) D. H. Macartney, C. A. Wadding, *Inorg. Chem.* **1994**, *33*, 5912.
- [21] M. Fujita, M. Aoyagi, K. Ogura, *Inorg. Chim. Acta* **1996**, *246*, 53.
- [22] M. Fujita, J. Yazaki, K. Ogura, *Chem. Lett.* **1991**, 1031.

Received: January 29, 2008